Journal of Arrhythmia 31 (2015) 101–107

Contents lists available at ScienceDirect

Journal of Arrhythmia

journal homepage: www.elsevier.com/locate/joa

Original Article

Spatial and temporal variability of the complex fractionated atrial electrogram activity and dominant frequency in human atrial fibrillation

Rikitake Kogawa, MD, Yasuo Okumura, MD*, Ichiro Watanabe, MD, Masayoshi Kofune, MD, Koichi Nagashima, MD, Hiroaki Mano, MD, Kazumasa Sonoda, MD, Naoko Sasaki, MD, Kimie Ohkubo, MD, Toshiko Nakai, MD, Atsushi Hirayama, MD

Division of Cardiology, Department of Medicine, Nihon University School of Medicine, Ohyaguchi-kamicho, Itabashi-ku, Tokyo 173-8610, Japan

ARTICLE INFO

Article history:
Received 16 May 2014
Received in revised form
30 July 2014
Accepted 5 August 2014
Available online 26 September 2014

Keywords:
Complex fractionated atrial electrogram
Dominant frequency
Basket catheter
Atrial fibrillation

ABSTRACT

Background: The presence of complex fractionated atrial electrograms (CFAEs) and high dominant frequencies (DFs) during atrial fibrillation (AF) have been demonstrated to be related to AF maintenance. Therefore, sequential mapping of CFAEs and DFs have been used for target sites of AF ablation. However, such mapping strategies are valid only if the CFAEs and DFs are spatiotemporally stable during the mapping procedure. We obtained spatially stable multi-electrode recordings to assess the spatiotemporal stability of CFAEs and DFs.
Methods: We recorded electrical activity during AF for 10 min with a 64-electrode basket catheter (48 bipole electrode pairs) placed in the left atrium in 36 patients with AF (paroxysmal AF [PAF], $n=16$; persistent AF [PerAF], $n=20$). The spatial and temporal distribution of the CFAEs (fractionation interval <120 ms) and high DFs (>8 Hz) at 1-min intervals for 10 min were compared for each of the 48 bipoles.
Results: The baseline CFAEs were located at $68.5\pm14.0\%$ (32.9 ± 6.7) of the 48 bipoles; however, the high DF sites were fewer ($9.6\pm8.6\%$ [4.6 ± 4.1 bipoles]). The CFAEs sites did not change significantly during the 10-min recording period (kappa statistic: 0.71 ± 0.24); however, the high DF sites changed significantly (kappa statistic: 0.07 ± 0.19). These spatiotemporal changes in the CFAEs and high DFs did not differ between patients with PAF and PerAF.
Conclusions: Regardless of the AF type, CFAEs sites, but not high DF sites, showed a high degree of spatial and temporal stability.

1. Introduction

Over the past decade, catheter-based pulmonary vein isolation (PVI) has become a widely accepted therapy for patients with symptomatic drug-refractory atrial fibrillation (AF) [1]. Termination of persistent AF (PerAF), however, often requires extensive ablation including ablation at complex fractionated atrial electrogram (CFAE) sites and high dominant frequency (DF) sites and/or multiple linear ablations in addition to the PVI [2–5]. CFAE and/or high DF sites have been shown to be effective targets for AF termination, thus suggesting their importance in the maintenance of AF [2–9]. Electrogram-based ablation has been used for an additive ablation strategy based on the hypothesis that critical CFAEs and high DFs are spatiotemporally stable. Nonetheless, it remains unclear whether the location of these electrical activities will be stable or variable at different time points while creating 3-dimensional (3D) maps, as the electrographic signals are sequentially recorded from a roving multipolar catheter. Simultaneous recordings from multiple sites at different time points are the only means by which we can evaluate the spatial and temporal distribution of CFAEs and high DFs. Therefore, we investigated the spatial and temporal distribution of CFAEs and high DFs in the left atrium (LA) during AF with the use of a multi-electrode basket catheter.

Abbreviations: AF, atrial fibrillation; CFAE, complex fractionated atrial electrogram; DF, dominant frequency; FI, fractionation interval; LA, left atrium; LAA, left atrial appendage; LV, left ventricle; MAP, monophasic action potential; PerAF, persistent AF; PV, pulmonary vein; PVI, pulmonary vein isolation; 3D, 3-dimensional

* Corresponding author. Tel.: +81 3 3972 8111; fax: +81 3 3972 1098.
E-mail address: yasuwo128@yahoo.co.jp (Y. Okumura).

2. Material and methods

2.1. Study patients

The current study consisted of 36 consecutive patients (35 men and 1 woman; mean age 56.9 ± 10.7 years) scheduled for their first

http://dx.doi.org/10.1016/j.joa.2014.08.004
1880-4276/

catheter ablation of AF. Sixteen had paroxysmal AF (PAF, i.e., AF lasting <7 days), and 20 had PerAF (i.e., AF lasting ≥ 7 days). Patients with cardiomyopathy, valvular heart disease, or congenital heart disease were excluded from the study. Adequate oral anticoagulation therapy was given for at least 1 month before the ablation procedure, and all antiarrhythmic drugs were discontinued for at least 5 half-lives before the procedure. Upon admission, transesophageal and transthoracic echocardiography were performed, and the baseline echocardiographic values were obtained: maximum LA volume by the prolate-ellipsoid method and left ventricular (LV) ejection fraction by the Teichholz method. The study protocol was approved by the Institutional Review Board of Nihon University Itabashi Hospital (December 7, 2012, RK-121109-5), and all patients provided written informed consent for their participation.

2.2. Electrophysiologic study

Electrophysiologic studies were performed with patients under conscious sedation achieved with propofol and fentanyl, as described previously [9,10]. After vascular access was obtained, a single transseptal puncture was performed, and intravenous heparin was administered to maintain an activated clotting time of >300 s. After 2 long sheaths (1 SL0 sheath and 1 Agilis sheath; St. Jude Medical, Inc., St. Paul, MN, USA) were inserted into the LA via a transseptal puncture, the 3D geometry of the LA and 4 pulmonary veins (PVs) was reconstructed with the use of an EnSite NavX system (version 8.0, St. Jude Medical, Inc.) and a 20-pole circular mapping catheter with 1.5-mm interelectrode spacing (Livewire Spiral HP catheter, St. Jude Medical, Inc.). To record the multiple bipolar signals (filter setting, 30–500 Hz) simultaneously, we used a multi-electrode basket catheter (Constellation, EP Technologies/Boston Scientific Corporation, San Jose, CA, USA), which consisted of 8 splines (A–H), each with 8 1-mm electrodes. The basket catheter was deployed in the LA, and the distal end was placed at the left PV antrum as shown in Fig. 1. Therefore, the basket catheter enabled us to record bipolar signals at the LA sectioned as follows: the posterior wall and roof of the LA and the LA appendage (LAA) ridge. A basket catheter of adequate size (38 mm with interelectrode spacing of 3 mm, 48 mm with interelectrode spacing of 4 mm, or 60 mm with interelectrode spacing of 5 mm) was chosen for consistent contact with the LA endocardium. If the patient was in sinus rhythm, AF was induced by rapid atrial pacing from the coronary sinus ostium for recording of the CFAEs and DFs.

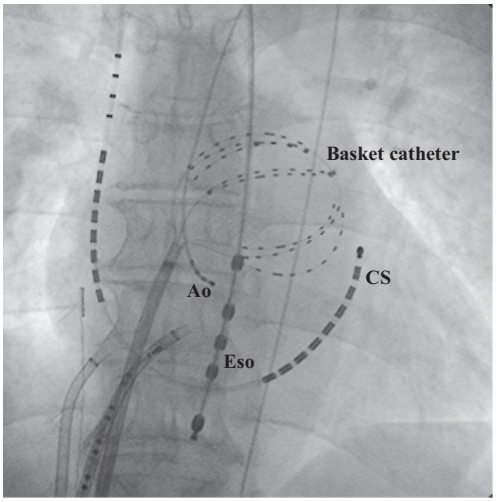

Fig. 1. Fluoroscopic view (anteroposterior projection) of the basket catheter position. The catheter is positioned at the anterolateral left atrium. *Ao*: catheter placed at the non-coronary cusp, *CS*: coronary sinus catheter, *Eso*: esophagus temperature catheter.

2.2.1. Bipolar signal recordings

Because of the limits on the number of electrodes that can be recorded by the EnSite system (version 8.0), the signals from 1 proximal electrode of each spline of the basket catheter could not be recorded. Thus, 6 bipole pairs from 7 electrodes at each spline totaling 48 bipoles (6 pairs $\times$ 8 splines) were entered into the analysis. With the basket catheter sitting in a stable position, the baseline bipolar signals were recorded for 5 s during AF from each bipolar electrode of the 48 bipoles and stored in the NavX mapping system. Thereafter, bipolar signals were recorded for 5 s at 1-min intervals for 10 min. All bipolar electrograms were analyzed offline on the NavX mapping system, and the mean numbers of CFAE and DF sites at the different recording times were compared.

2.2.2. Fast Fourier transform (FFT) analysis

For the FFT analysis, the distribution of the DF sites was analyzed by the DF software installed in the NavX mapping system (sampling rate, 1200 Hz; resolution, 0.14 Hz; low-pass filter, 20-Hz; high-pass filter, 1-Hz with a Hamming window function) as previously reported [9–12]. Five-second bipolar signals recorded during AF were used for the DF analysis. A high DF site was defined as a site with a frequency of >8 Hz. The regularity index was taken as the area within the 0.75-Hz band around the DF divided by the area of the frequencies sampled from 3 Hz to 14 Hz [8]. A regularity index of <0.2 was excluded from the analysis.

2.3. CFAE analysis

For the CFAE analysis, the NavX mapping parameters were set to the CFAE-mean, an algorithm was used to determine the average index of the fractionation at each site, and a color map of the fractionation intervals (FIs) (CFAE map) was constructed [9–12]. The FI was taken as the average time between consecutive deflections at 5-s recording periods. The settings included a refractory period of 40 ms, peak-to-peak sensitivity between 0.05 mV and 0.1 mV, and each electrogram duration of <10 ms. Continuous CFAEs were defined as having a mean FI of <50 ms and variable CFAEs as having FIs of 50–120 ms.

2.4. Statistical analysis

Continuous variables are expressed as the mean $\pm$ SD or median and interquartile ranges. When values were skewed, the Mann–Whitney *U* test was used to analyze the differences in the variables between the patients with PAF and those with PerAF. When the values were normally distributed, between-group differences were analyzed by Student's *t* test. A Fisher's exact probability test was used to compare the distribution of the dichotomous variables between the 2 groups. Agreement between the locations of high DF sites and CFAE sites at each segment of the basket catheter was assessed by the kappa statistic, which was calculated by subtracting the proportion of readings expected to agree by chance, i.e., P_e, from the overall agreement, P_o, and dividing the remainder by the proportion of readings not expected to agree by chance: $\text{kappa}=(P_o-P_e)/(1-P_e)$. The kappa statistics range from -1.0 to $+1.0$, with 0 indicating a chance agreement and $+1.0$ indicating a perfect agreement. Kappa values >0.75 indicated an excellent agreement, values 0.40–0.75 indicated a fair-to-good agreement, and values <0.4 indicated a poor agreement [10]. *P* values <0.05 were considered statistically significant. All statistical analyses were performed with JMP 8 software (SAS Institute, Cary, NC, USA).

3. Results

3.1. Baseline clinical characteristics and echocardiographic values

The baseline clinical characteristics and echocardiographic values are shown for all patients and for patients per group in Table 1. There were no statistical differences in the baseline clinical characteristics between the 2 groups. The LA dimension (36.9 ± 5.5 mm vs. 43.3 ± 6.8 mm, $P=0.0036$), LA volume (39.7 ± 14.4 vs. 62.0 ± 23.1 cm^3, $P=0.0015$), and end-systolic LV dimension (29.3 ± 4.7 vs. 34.7 ± 7.7 mm, $P=0.0167$) were significantly greater in the PerAF group than in the PAF group.

3.2. Distribution of the baseline CFAE and high DF sites

For the CFAE recordings, 44.0 ± 6.7 of the 48 bipolar signals (91.6 ± 3.2%) per patient were available for analysis. The remaining 4.0 ± 6.7 of the 48 bipole signals (8.4 ± 3.2%) per patient could not be used due to poor signal quality. For the DF recordings, 5.4 ± 10.3 of the 48 bipolar signals (11.3 ± 4.9%) per patient were of poor quality or had a regularity index of < 0.2, leaving 42.6 ± 10.3 of the 48 bipole signals (88.7 ± 4.9%) available for analysis. The baseline bipole signals representing CFAE sites accounted for 32.9 ± 6.7 of the total 48 bipoles (68.5 ± 14.0%). The number of CFAE sites was significantly greater in the patients with PAF than in the patients with PerAF (36.3 ± 5.3 [75.6 ± 11.1%] vs. 31.4 ± 5.7 [65.4 ± 11.9%] of the total 48 bipoles, $P=0.0202$). Regionally, there was no significant difference in the prevalence of CFAE sites between the LAA ridge and the LA roof (80.2 ± 14.2% vs. 70.5 ± 25.9%, $P=0.1364$); however, the prevalence of CFAE sites in the LAA ridge was significantly greater than that in the LA posterior wall (80.2 ± 14.2% vs. 59.3 ± 19.9%, $P<0.0001$). The baseline prevalence of a high DF, which was calculated as the number of bipole signals indicating high DF sites out of the total 48 bipoles, was 4.6 ± 4.1 bipoles (9.6 ± 8.6%). The number of high DF sites was significantly greater in the patients with PAF than in the patients with PerAF (5.6 ± 3.3 [11.6 ± 6.8%] vs. 3.1 ± 1.8 [6.5 ± 3.8%] bipoles, $P=0.0137$). Regionally, there was no significant difference in the prevalence of high DF sites among the LAA ridge, the LA roof, and the LA posterior wall (15.9 ± 20.2% vs. 10.0 ± 17.1% vs. 11.1 ± 12.0%: LAA ridge vs. LA roof, $P=0.1501$; LAA ridge vs. LA posterior wall; $P=0.3358$; LA roof vs. LA posterior wall, $P=0.6669$). Only 4.3 ± 4.5 bipoles (9.0 ± 9.3%) overlapped between the CFAE and high DF sites.

3.3. Spatiotemporal distribution of CFAEs

An example of a change in the distribution of the CFAE sites over 10 min is shown in Fig. 2. The concordance between the CFAE sites was 89.3 ± 11.9%, and the difference was 10.7 ± 11.9% between the sites on the baseline maps and the sites on the maps obtained subsequently at each time point during the10-min recording period. Thus, the CFAE sites recorded from each bipolar electrode were stable over the 10-min period, as demonstrated by the kappa statistics (average kappa value between the maps at baseline vs. the maps at each time point: 0.71 ± 0.24; Table 2). There was no difference between the patients with PAF and PerAF regarding the agreement between the CFAE sites over the 10-min recording period (average kappa values: 0.70 ± 0.20 and 0.71 ± 0.27, respectively; $P=0.1848$). Furthermore, a regional difference was found in the spatiotemporal distribution of CFAE sites. CFAE site stability at the LA roof, LA posterior wall, and LAA ridge as shown by average kappa values was 0.59 ± 0.04, 0.69 ± 0.05, and 0.76 ± 0.08, respectively (LAA ridge vs. LA roof; $P<0.0001$, LAA ridge vs. LA posterior, $P<0.0001$; LA roof vs. LA posterior, $P<0.0001$).

3.4. Spatiotemporal distribution of the DFs

An example of a change in the distribution of the DF sites over the 10-min recording period is shown in Fig. 3. Over the 10-min recording period, the concordance between the high DF sites was 18.1 ± 24.7%, with a difference of 81.9 ± 24.7% between the baseline distribution and the distribution at each time point. Overall, the high DF sites changed markedly, as demonstrated by the lack of agreement between the high DF sites over the 10-min recording period (average kappa value between the maps at baseline vs. the maps at each time point: 0.07 ± 0.19; Table 2). There was no difference between patients with PAF and PerAF regarding the agreement between the high DF sites over the 10-min recording period (average kappa values: 0.09 ± 0.22 and 0.08 ± 0.17, respectively; $P=0.2821$). There was no difference in the spatiotemporal distribution of high DF sites between the LAA ridge, LA roof, and LA posterior wall (average kappa values: 0.13 ± 0.09 vs. 0.11 ± 0.09

Table 1
Baseline clinical characteristics and echocardiographic variables in all patients and per study group.

	All ($n=36$)	**PAF** ($n=16$)	**PerAF** ($n=20$)	***P*-value**[a]
Age, years	56.9 ± 10.7	57.6 ± 12.1	56.3 ± 9.5	0.7184
Sex, male	35 (97.2)	16 (100)	19 (95.0)	0.2628
AF duration, days	690 (375–1800)	570 (450–1800)	675 (307–1627)	0.2729
Body mass index, kg/m^2	25.8 ± 4.0	25.4 ± 4.8	26.1 ± 3.1	0.5884
Casual factors				
Hypertension	19 (52.8)	7 (43.8)	11 (55.0)	0.5153
Diabetes mellitus	4 (11.1)	2 (12.5)	2 (10.03)	0.9061
Prior stroke	4 (11.1)	1 (6.3)	3 (15.0)	0.3335
Heart failure	5 (19.4)	3 (18.8)	4 (20.0)	0.7963
TTE measures				
LAD (mm)	40.3 ± 6.2	36.9 ± 5.5	43.3 ± 6.8	0.0036
LAV (cm^3)	51.7 ± 19.6	39.7 ± 14.4	62.0 ± 23.1	0.0015
LVDd (mm)	49.2 ± 5.9	47.1 ± 5.7	51.0 ± 6.0	0.0528
LVDs (mm)	32.2 ± 6.5	29.3 ± 4.7	34.7 ± 7.7	0.0167
LVEF (%)	64.1 ± 10.5	67.8 ± 6.6	61.0 ± 13.0	0.0601

PAF = paroxysmal AF; PerAF = persistent AF; TTE = transthoracic echocardiography; LAD = left atrial dimension; LAV = left atrial volume; LVDd = left ventricular end-diastolic dimension; LVDs = left ventricular end-systolic dimension; LVEF = left ventricular ejection fraction.

[a] PAF vs. PerAF group.

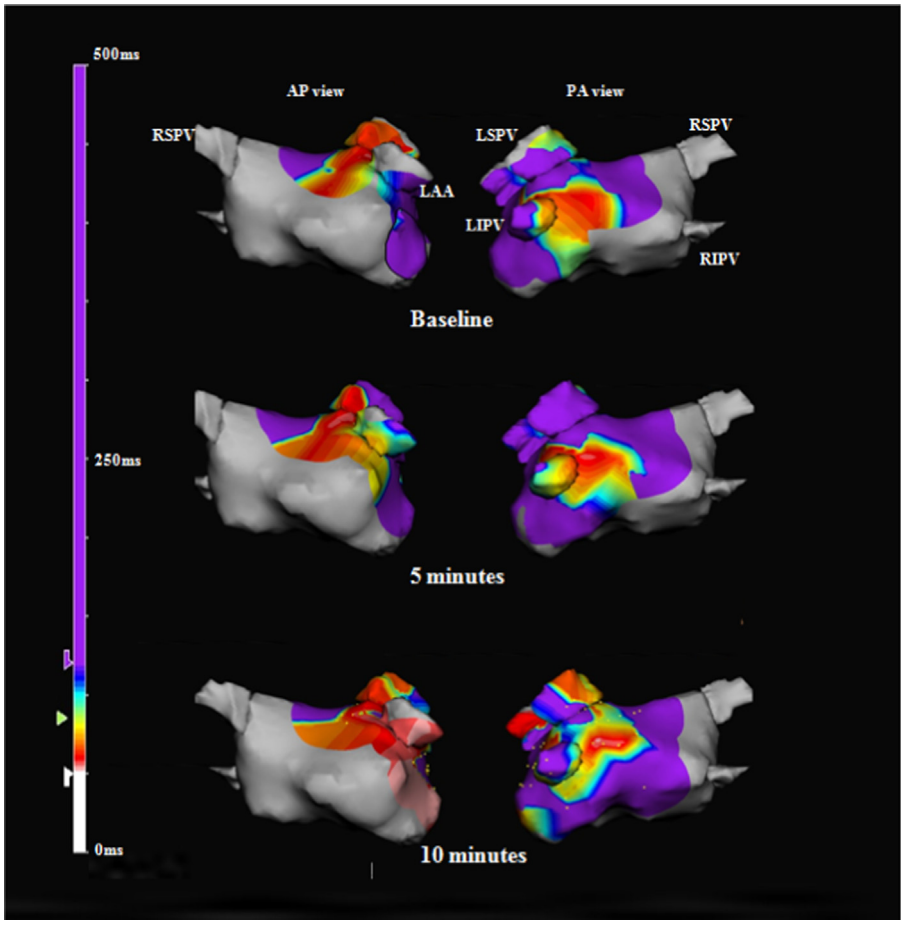

Fig. 2. Representative complex fractionated atrial electrogram (CFAE) maps created over 10 min on the NavX 3-dimensional mapping system. The red areas are variable CFAE sites with a mean fractionated interval of 50–120 ms. Locations of the CFAE sites on the maps obtained at 5 and 10 min are similar to those on the baseline maps. *AP*: anteroposterior, *LAA*: left atrial appendage, *LIPV*: left inferior pulmonary vein, *LSPV*: left superior pulmonary vein, *PA*: posteroanterior, *RIPV*: right inferior pulmonary vein, *RSPV*: right superior pulmonary vein.

Table 2
The kappa value for the agreement of CFAE sites and high DF sites over 10 min.

	Kappa value	
	CFAE sites	**High DF sites**
1 min	0.76 ± 0.21	0.03 ± 021
2 min	0.75 ± 0.18	0.09 ± 0.23
3 min	0.74 ± 0.19	0.10 ± 0.19
4 min	0.75 ± 0.19	0.06 ± 0.16
5 min	0.79 ± 0.25	0.08 ± 0.17
6 min	0.69 ± 0.23	0.003 ± 0.10
7 min	0.68 ± 0.27	0.08 ± 0.17
8 min	0.68 ± 0.26	0.07 ± 0.17
9 min	0.67 ± 0.26	0.09 ± 0.21
10 min	0.71 ± 0.24	0.06 ± 0.25

vs.0.11 ± 0.10; LAA ridge vs. LA roof, $P=0.8457$; LAA ridge vs. LA posterior, $P=0.9219$; LA roof vs. LA posterior, $P=0.7695$).

4. Discussion

4.1. Major findings

We found that the spatial and temporal distribution of the CFAEs in the LA did not change over the 10-min recording period, but that there was significant variability in the high DFs. These findings did not differ between patients with PAF and PerAF.

4.2. Spatial and temporal changes in the CFAEs and high DFs

Previous studies demonstrated that the temporal distribution of the CFAE sites did not change over time [13–16]. Scherr et al. compared 149 CFAE sites and of 238 non-CFAE sites on the initial and repeat CFAE maps, and demonstrated that 135 (90.6%) and 225 (94.5%) remained as CFAE and non-CFAE sites, respectively [13]. In addition, Verma et al. reported no significant changes in the AF cycle length in the LA or in specific regions of the LA over a 20-min period [14]. Roux et al. showed both qualitatively and quantitatively that the CFAE regions were relatively stable over time, with a 78% concordance and a 17.5 ± 9.4% difference between the CFAE maps created 31 min apart [16]. In these prior studies, all CFAE maps were sequentially created by roving catheters [13–16]. Therefore, the mapping points analyzed between the different time points may or may not have been identical, and the signals were recorded at slightly different time points due to the time required to create the maps. On the other hand, our simultaneous 3D mapping achieved with the basket catheter showed that 89.3 ± 11.9% of CFAEs were spatiotemporally stable and that only 10.7 ± 11.9% differed between the baseline CFAE map and the maps obtained during the 10-min recording period. We further evaluated the spatiotemporal agreement in detail on the basis of kappa statistics and found a fair-to-good agreement. The pathogenesis of the CFAEs has been attributed to various electrophysiologic mechanisms, e.g., slowed conduction, dyssynchronous activation of separate cell groups at pivot points, and local reentry circuits or sites of neurotransmitter release from autonomic

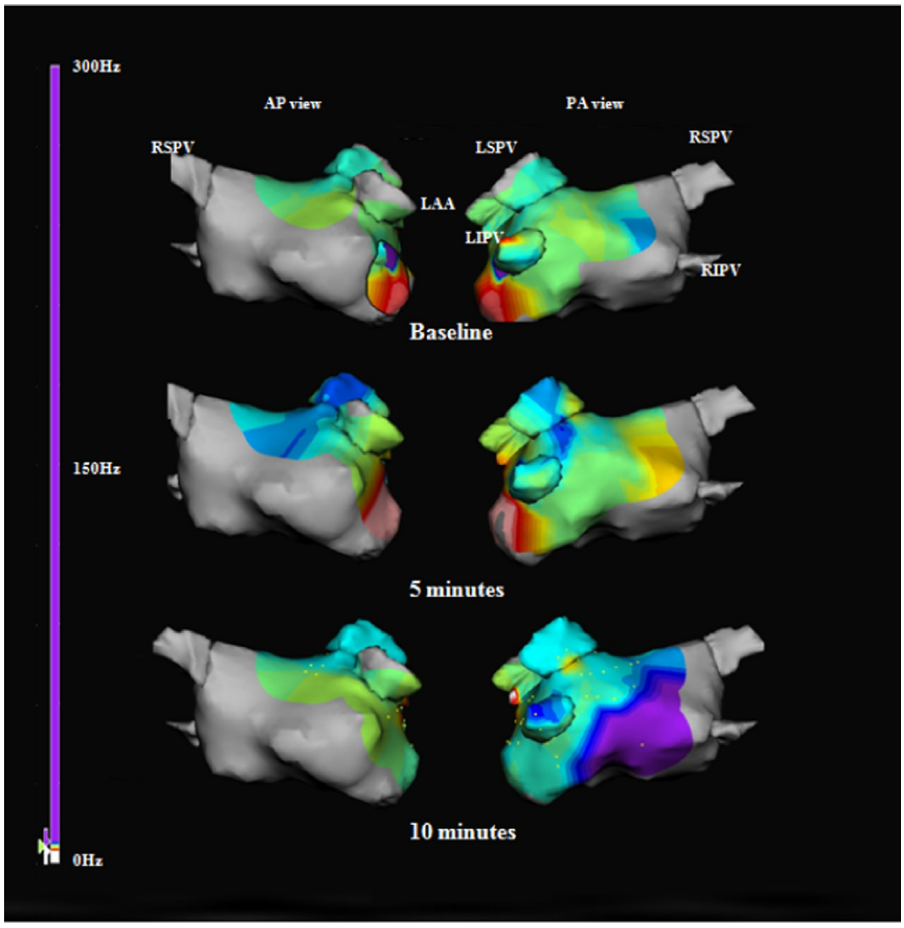

Fig. 3. Representative dominant frequency (DF) maps created over 10 min on the NavX 3-dimensional mapping system. The bright purple areas are high DF sites with frequencies of >8 Hz. The locations of the high DF sites on the maps obtained at 5 and 10 min are entirely different from the locations on the baseline maps. The abbreviations are as in Fig. 2.

ganglionated plexi [17-20]. Other contributing mechanisms include tissue anisotropy, far-field potentials, wave collisions, wave breaks, sites in very close proximity to focal driver activity, and passively activated regions [2,5–7,9–12]. Some of these mechanisms may occur at fixed sites, whereas other mechanisms are complex and unstable, and may vary over time. Our data were consistent with previous data suggesting that stable, fixed CFAE sites may be critical targets for AF ablation. However, the stable CFAE sites we identified accounted for approximately 90% of the total recording sites, which is a greater percentage than suggested in recent studies [17,18]. This may be due to the limited recording area covered by the basket catheter in the current study, i.e., the LA roof, LAA ridge, and LA posterior. These are known to be areas where CFAEs have been recorded predominantly and consistently [6,9,16]. In fact, a greater prevalence of CFAE sites in the LAA ridge at baseline led to an increase in kappa value. Narayan et al. sought to investigate the mechanism underlying CFAEs by using monophasic action potentials (MAPs) and reported that 67% of CFAE sites showed nonlocal (far-field) signals (67%), and that the remaining sites showed pansystolic local activity (localized AF source) (8%) and CFAE activity after AF acceleration, often with MAP alternans (8%) [17]. Taken together, the stable CFAE sites represented by our data would have overestimated the critical sources of AF maintenance.

In contrast to the spatiotemporal stability of the CFAEs, the high DF sites changed over time. High DFs have been reported to be related to the center of a focal-firing rotor or local reentry circuit, based mainly on data obtained from animal studies. Human studies have supported this mechanistic insight [8–12]. A human study based on focal impulses and rotor mapping concluded that 2.3 ± 1.1 of localized AF rotors or focal sources were located at or near the PVs (22.8%), LA roof (16.0%), and elsewhere in the left (28.2%) and right (33.0%) atria [21]. If all or most high DF sites represent localized AF rotors or focal sources, the high DF sites would be stable and could be critical sites for AF ablation. However, we found instability of the high DF sites. Our data can be explained by the hypothesis positing that AF rotors move spatiotemporally. A noninvasive electrocardiographic imaging study of continuous biatrial epicardial activation sequences of AF in humans revealed rotor activity to be rare (15%), and the patterns seemed transient, whereas the most common patterns of AF were multiple wavelets (92%), with focal PV (69%) and non-PV (62%) activity [22]. Furthermore, the findings that DFs are significantly affected by variations in the cycle length, amplitude, and morphology, such as split or double potentials [23-25] are additional factors causing changes in the high DF sites. In addition, high DF sites were distributed around the PVs, but not in the LA, in patients with PAF, whereas in patients with PerAF or long-lasting AF, more high DFs sites were distributed toward the LA and were complicated [9,11]. Therefore, limited recordings from the roof and posterior LA, and the LAA ridge by the basket catheter may have missed the critical, fixed high DF sites located at the other PVs or other LA sites. It is important to note that our results were consistent with the results of several previous studies. Habel et al. demonstrated the spatiotemporal distribution of the DF sites by continuous recording with a basket catheter, and concluded

that the DF sites varied over 5 min [26]. A study of simultaneous noncontact electrogram recordings revealed that focal areas of high DFs were more common in patients with PAF than with PerAF, and that the DFs were spatiotemporally unstable and were not the source of centrifugal activation [27]. Therefore, high DF sites were not indicative of fixed drivers of AF. These limitations on the high DF sites may explain why DF-guided ablation in patients with PerAF fails to produce a better outcome beyond that achieved with PVI alone [28]. These phenomena may be the keys to the results that the high DF sites show spatiotemporal variations and may not serve as critical targets for AF ablation.

We also showed that there were no significant differences in the spatiotemporal distribution of CFAEs and high DFs between patients with PAF and PerAF. Theoretically, the mechanisms of AF maintenance may differ between PAF and PerAF, as suggested by previous studies that demonstrated the spatiotemporal differences in CFAE activity and high DFs between patients with PAF and PerAF [9,11,21,27]. Patients with PAF had more stable AF sources clustered around the PVs [15]. An absence of characteristic differences between the AF types may be due to a limited mapping area where CFAE and DF sites are consistently recorded regardless of PAF or PerAF [6,9,16]. The lack of recording sites within the PV in the current study may explain these results. Eric et al. demonstrated that the basket catheter leaves nearly 50% of the endocardial LA surface unmapped [29].

Regarding the relationship between CFAE and high DF, we found only 9% overlap between the two parameters. Previous reports have suggested that both CFAEs and high DFs were closely related and thus play an important role in the maintenance of AF circuits [4,5,21]. However, other reports have shown that these parameters correlated poorly [24,25]. Our findings of widely distributed and spatiotemporally stable CFAE sites with meandering high DF sites, a similar distribution between patients with PAF and PerAF, and little overlap of CFAE and DF sites highlight the limitations of recording CFAE activity and/or DFs for determining critical sites of AF maintenance. Therefore, more sophisticated spectral analysis techniques, such as focal impulse and rotor mapping using phase analysis, may be necessary to guide AF ablation procedures [21,22].

4.3. Study limitations

The current study was subject to several limitations. First, the surface contact posed a technical limitation. Frequently, it was not possible to make endocardial contact with all of the electrodes. Second, the CFAE and DF sites were identified by means of a special algorithm installed in the NavX mapping system. Third, the area covered by the basket catheter was methodically quite restricted and posed a major limitation regarding the assessment for DF, as DF is the parameter representing the relatively dominant frequency of an entire atrium. The limited recording area also cast doubt on whether our findings would apply to other sites, including the right atrium or septal LA sites. Finally, we did not address whether CFAE or high DF sites served as critical sites for AF perpetuation by ablating these sites. Rather, we simply provided new data for understanding the electrophysiologic properties of CFAEs and DFs.

5. Conclusions

CFAEs sites, but not high DF sites, show a high degree of spatial and temporal stability during AF.

Conflict of interest

There is no financial conflict of interest.

Acknowledgments

We would like to thank MS. Wendy Alexander-Adams for linguistic assistance in the preparation of this manuscript.

References

[1] Wazni O, Wilkoff B, Saliba W. Catheter ablation for atrial fibrillation. N Engl J Med 2011;365:2296–304.
[2] Nademanee K, McKenzie J, Kosar E, et al. A new approach for catheter ablation of atrial fibrillation: mapping of electrophysiologic substrate. J Am Coll Cardiol 2004;43:2044–53.
[3] Haïssaguerre M, Sanders P, Hocini M, et al. Catheter ablation of long-lasting persistent atrial fibrillation: critical structures for termination. J Cardiovasc Electrophysiol 2005;16:1125–37.
[4] O'Neill MD, Jaïs P, Takahashi Y, et al. The stepwise ablation approach for chronic atrial fibrillation-evidence for a cumulative effect. J Interv Card Electrophysiol 2006;16:153–67.
[5] Schmitt C, Estner H, Hecher B, et al. Radiofrequency ablation of complex fractionated atrial electrograms (CFAE): preferential sites of acute termination and regularization in paroxysmal and persistent atrial fibrillation. J Cardiovasc Electrophysiol 2007;18:1039–46.
[6] Atienza F, Calvo D, Almendral J, et al. Mechanisms of fractionated electrograms formation in the posterior left atrium during paroxysmal atrial fibrillation in humans. J Am Coll Cardiol 2011;57:1081–92.
[7] Gerstenfeld EP, Lavi N, Bazan V, et al. Mechanism of complex fractionated electrograms recorded during atrial fibrillation in a canine model. Pacing Clin Electrophysiol 2011;34:844–57.
[8] Takahashi Y, Sanders P, Jaïs P, et al. Organization of frequency spectra of atrial fibrillation: relevance to radiofrequency catheter ablation. J Cardiovasc Electrophysiol 2006;17:382–8.
[9] Okumura Y, Watanabe I, Kofune M, et al. Characteristics and distribution of complex fractionated atrial electrograms and the dominant frequency during atrial fibrillation: relationship to the response and outcome of circumferential pulmonary vein isolation. J Interv Card Electrophysiol 2012;34:267–75.
[10] Nagashima K, Okumura Y, Watanabe I, et al. Does location of epicardial adipose tissue correspond to endocardial high dominant frequency or complex fractionated atrial electrogram sites during atrial fibrillation? Circ Arrhythm Electrophysiol 2012;5:676–83.
[11] Lin YJ, Tai CT, Kao T, et al. Spatiotemporal organization of the left atrial substrate after circumferential pulmonary vein isolation of atrial fibrillation. Circ Arrhythm Electrophysiol 2009;2:233–41.
[12] Lin YJ, Tsao HM, Chang SL, et al. Role of high dominant frequency sites in nonparoxysmal atrial fibrillation patients: insights from high-density frequency and fractionation mapping. Heart Rhythm 2010;7:1255–62.
[13] Scherr D, Dalal D, Cheema A, et al. Long- and short-term temporal stability of complex fractionated atrial electrograms in human left atrium during atrial fibrillation. J Cardiovasc Electrophysiol 2009;20:13–21.
[14] Verma A, Wulffhart Z, Beardsall M, et al. Spatial and temporal stability of complex fractionated electrograms in patients with persistent atrial fibrillation over longer time periods: relationship to local electrogram cycle length. Heart Rhythm 2008;5:1127–33.
[15] Lin YJ, Tai CT, Kao T, et al. Consistency of complex fractionated atrial electrograms during atrial fibrillation. Heart Rhythm 2008;5:406–12.
[16] Roux JF, Gojraty S, Bala R, et al. Complex fractionated electrogram distribution and temporal stability in patients undergoing atrial fibrillation ablation. J Cardiovasc Electrophysiol 2008;19:815–20.
[17] Narayan SM, Wright M, Derval N, et al. Classifying fractionated electrograms in human atrial fibrillation using monophasic action potentials and activation mapping: evidence for localized drivers, rate acceleration, and nonlocal signal etiologies. Heart Rhythm 2011;8:244–53.
[18] Narayan SM, Shivkumar K, Krummen DE, et al. Panoramic electrophysiological mapping but not electrogram morphology identifies stable sources for human atrial fibrillation: stable atrial fibrillation rotors and focal sources relate poorly to fractionated electrograms. Circ Arrhythm Electrophysiol 2013;6:58–67.
[19] Katritsis D, Sougiannis D, Batsikas K, et al. Autonomic modulation of complex fractionated atrial electrograms in patients with paroxysmal atrial fibrillation. J Interv Card Electrophysiol 2011;31:217–23.
[20] Katritsis D, Giazitzoglou E, Sougiannis D, et al. Complex fractionated atrial electrograms at an atomic sites of ganglion at edplexiinatrial fibrillation. Europace 2009;11:308–15.
[21] Narayan SM, Krummen DE, Shivkumar K, et al. Treatment of atrial fibrillation by the ablation of localized sources: CONFIRM (Conventional Ablation for Atrial Fibrillation With or Without Focal Impulse and Rotor Modulation) trial. J Am Coll Cardiol 2012;60:628–36.

[22] Cuculich PS, Wang Y, Lindsay BD, et al. Noninvasive characterization of epicardial activation in humans with diverse atrial fibrillation patterns. Circulation 2010;122:1364–72.
[23] Ng J, Kadish AH, Goldberger JJ. Effect of electrogram characteristics on the relationship of dominant frequency to atrial activation rate in atrial fibrillation. Heart Rhythm 2006;3:1295–305.
[24] Elvan A, Linnenbank AC, van Bemmel MW, et al. Dominant frequency of atrial fibrillation correlates poorly with atrial fibrillation cycle length. Circ Arrhythm Electrophysiol 2009;2:634–44.
[25] Singh SM, Heist EK, Koruth JS, et al. The relationship between electrogram cycle length and dominant frequency in patients with persistent atrial fibrillation. J Cardiovasc Electrophysiol 2009;20:1336–42.
[26] Habel N, Znojkiewicz P, Thompson N, et al. The temporal variability of dominant frequency and complex fractionated atrial electrograms constrains the validity of sequential mapping in human atrial fibrillation. Heart Rhythm 2010;7:586–93.
[27] Jarman JW, Wong T, Kojodjojo P, et al. Spatiotemporal behavior of high dominant frequency during paroxysmal and persistent atrial fibrillation in the human left atrium. Circ Arrhythm Electrophysiol 2012;5:650–8.
[28] Verma A, Lakkireddy D, Wulffhart Z, et al. Relationship between complex fractionated electrograms (CFE) and dominant frequency (DF) sites and prospective assessment of adding DF-guided ablation to pulmonary vein isolation in persistent atrial fibrillation (AF). J Cardiovasc Electrophysiol 2011;22:1309–16.
[29] Eric FB, Rich N, Peyman B, et al. Does the 64-pole basket catheter provide adequate spatial coverage and electrode contact for mapping atrial fibrillation in humans? Heart Rhythm 2014;5:S20.